Tectonophysics xxx (2009) xxx–xxx

Contents lists available at ScienceDirect

Tectonophysics

journal homepage: www.elsevier.com/locate/tecto

Crustal structures in the area of the 2008 Sichuan earthquake from seismologic and gravimetric data

A. Robert [a,*], J. Zhu [b], J. Vergne [c], R. Cattin [d], L.S. Chan [e], G. Wittlinger [c], G. Herquel [c], J. de Sigoyer [a], M. Pubellier [a], L.D. Zhu [b]

[a] Laboratoire de Géologie de l'Ecole Normale Supérieure, CNRS-UMR 8538, Paris, France
[b] Chengdu University of Technology, Chengdu, China
[c] Institut de Physique du Globe de Strasbourg, Ecole et Observatoire des Sciences de la Terre, CNRS-UMR 7516, Université Louis Pasteur, Strasbourg, France
[d] Geoscience Montpellier, CNRS-UMR 5243, Montpellier, France
[e] Department of Earth Sciences, The University of Hong-Kong, Hong-Kong, China

ARTICLE INFO

Article history:
Received 5 May 2009
Received in revised form 10 November 2009
Accepted 13 November 2009
Available online xxxx

Keywords:
Longmen Shan
Crustal structures
Receiver functions
Gravity modelling

ABSTRACT

The 12 May 2008 the Sichuan earthquake was one of the worst natural disasters in China. Here, we present a detailed picture of the epicentral area inferred geophysical data. Based on the analysis of teleseismic data acquired by a dense seismic network, we highlight an abrupt 20 km Moho offset between the Sichuan Basin and the Tibetan plateau and a horizontal discontinuity at ~15 km depth, which may connect with the ruptured zone of the 2008 event. We obtain low mean crustal velocity ratios, which suggest the absence of a thick and extensive zone of partial melt within the crust beneath the eastern part of the Songpan–Garze Terrane. All our data support the idea that the Longmen Shan range mark a zone of active strain localization due to the rigid Yangtze craton resisting eastward displacement of the Tibetan Plateau.

1. Introduction

The 12 May 2008 Mw = 7.9 the Wenchuan earthquake on the western margin of the Sichuan Basin is arguably the largest intracontinental earthquake in western China ever recorded by instruments. InSAR data and field observations (Stone, 2008; Xu et al., 2009; De Michele et al., in press) suggest an oblique thrusting and segmented rupture. The Guanxian–Beichuan–Wenchuan faults system structures the Longmen Shan belt, which limits the actively deforming Tibetan plateau to the west and the stable Yangtze craton to the east (Fig. 1). A first glance at this major earthquake suggests a typical event that accommodates regional shortening between two blocks through a sudden release of the stresses accumulated on a frontal thrust fault. However, this earthquake occurred on a very peculiar margin of the Tibetan Plateau where high mountains and a very steep topographic gradient subsists despite almost no significant present day horizontal shortening (<3 mm yr^{-1}) as inferred from GPS measurements (Chen et al., 2000; Gan et al., 2007; Shen et al., 2009) and the lack of a developed Neogene sedimentary foreland in the Sichuan Basin (Richardson et al., 2008). Two main conceptual models for the uplift and the evolution since the Tertiary of the Longmen Shan range front are commonly proposed. The first one explains the uplift by faulting and crustal shortening (Tapponnier et al., 2001; Xu et al., 2009) whereas in the other model, the uplift is produced by the inflation of a ductile lower crust (Royden et al., 1997; Burchfiel et al., 2008). The last model does not require important long term horizontal shortening at the surface which is not the case of the brittle crustal thickening model. To study this intriguing margin we coupled several geophysical approaches in an integrated study of the Longmen Shan region since 2004. Hereafter we present a detailed image of the crustal structures in the epicentral region inferred from analysis of teleseismic data acquired by a dense seismic network and gravity measurements (Figs. 1 and 2), which together bring new constraints on the geodynamic context that led to the 12 May 2008 disastrous event.

2. Deep structures from seismological data

A dense network of 34 broad-band and intermediate-band seismic stations was deployed across the Longmen Shan range between November 2005 and March 2007, in the framework of a collaboration between the Institute of Technology of Chengdu (Chengdu, China), the Ecole Normale Supérieure (Paris, France) and the Institut de Physique du Globe (Strasbourg, France). The network is mostly constituted by a dense line of stations, with a mean inter-station distance of about 10 km ending at the Xianshuihe fault, and passing close to the epicentral zone of the 12 May 2008 earthquake (Fig. 1). Continuous data from 3-components sensors (Streikeisen STS2,

* Corresponding author. Laboratoire de Géologie - ENS, 24, rue Lhomond 75005, Paris Cedex 5, France.
E-mail address: arobert@geologie.ens.fr (A. Robert).

0040-1951/$ – see front matter © 2009 Elsevier B.V. All rights reserved.
doi:10.1016/j.tecto.2009.11.010

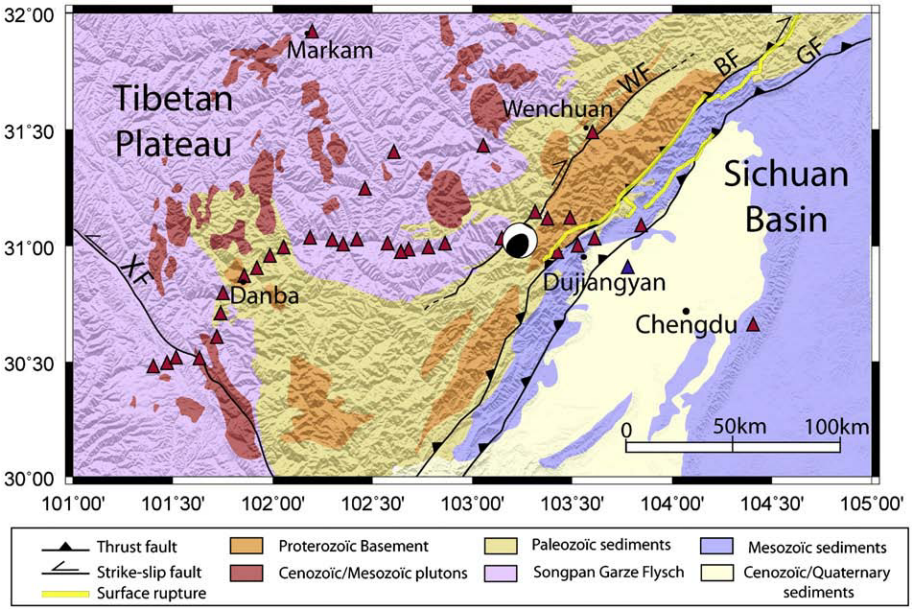

Fig. 1. Shaded relief map of the Longmen Shan region with major geological units and active faults: Guanxian (GF), Beichuan (BF), Wenchuan (WF) and Xianshuihe (XF). Red triangles give the location of the 33 temporary seismological stations installed between November 2005 and March 2007 and the blue triangle the Chengdu permanent station of the China Digital Seismic Network. Also shown is the focal mechanism of the 12 May 2008 (Mw = 7.9) earthquake reported by the US Geological Survey plotted at its epicentre and the surface rupture mapped by Xu et al. (2009).

Guralp CMG40T, Agecodagis NOEMAX and Lennartz LE3D5S) were recorded continuously with Reftek 130A and Agecodagis Titan recorders at a sample rate varying from 20 to 50 Hz.

A total of 8603 teleseismic records has been processed using the "receiver function" technique (Burdick and Langston, 1977) to isolate P to S converted waves produced at impedance (product of density and seismic velocity) discontinuities below each station. Pre-processing of the seismic data includes a correction of the instrument response, a rotation of the horizontal components according to the theoretical backazimuth, and a 0.05–1 Hz butterworth band-pass filtering, To produce a receiver function, the radial component is deconvolved from the vertical one following an iterative approach in the time domain (Ligorria and Ammon, 1999) using 100 iterations. Finally, an automatic selection of the receiver functions has been applied to reject the ones with a too low signal to noise ratio and 1222 receiver functions were selected. The receiver functions were migrated to depth using the common conversion point stacking technique (Dueker and Sheehan, 1998) to produce a cross section of the major crustal interfaces across the Longmen Shan and Eastern Tibet. This step requires a velocity model to project the time samples

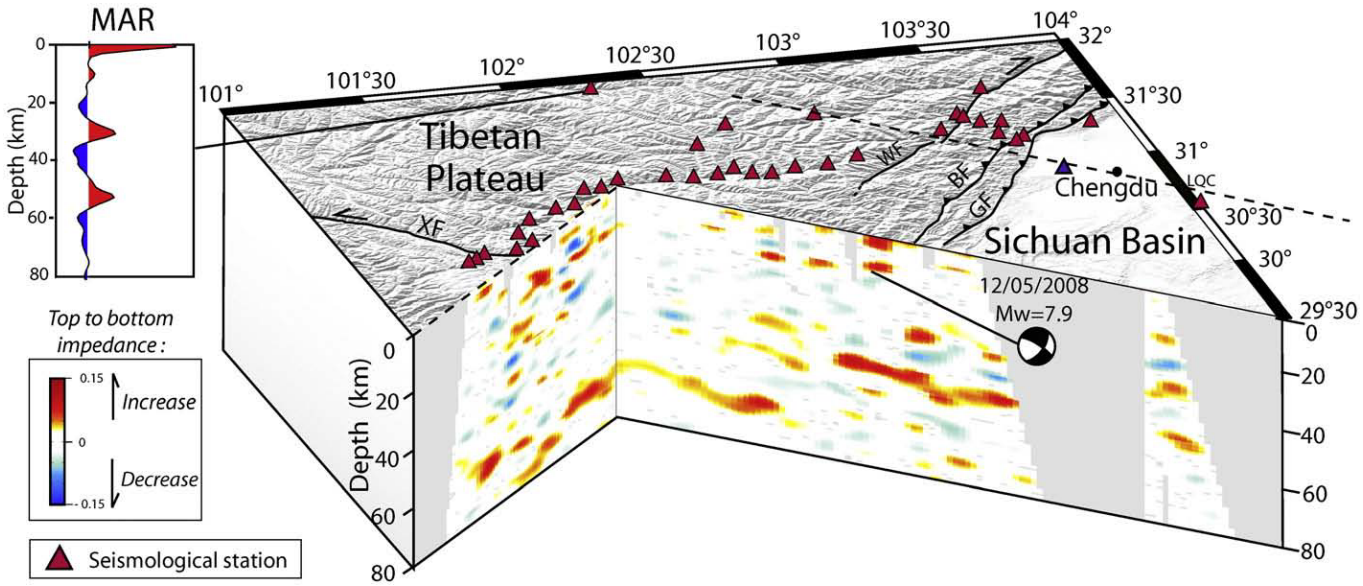

Fig. 2. Block diagram of the migrated radial receiver functions projected along two cross sections, indicated by the dashed lines, and running approximately perpendicular to the Longmen Shan front to the East and to the Xianshuihe fault to the West. The focal mechanism of the 12 May 2008 earthquake is represented along a vertical plane and indicated at the hypocenter location. Major interfaces with top to bottom increasing and decreasing impedance are represented by red and blue colors, respectively. Gray color represents area not sampled by seismic rays thus where the structure cannot be imaged. The Markam (MAR) station being out of profile, the stack of individually migrated receiver functions at this station is represented on the left.

Please cite this article as: Robert, A., et al., Crustal structures in the area of the 2008 Sichuan earthquake from seismologic and gravimetric data, Tectonophysics (2009), doi:10.1016/j.tecto.2009.11.010

of the receiver functions along the corresponding ray paths. We construct a 2D velocity model using the *P* velocities inferred from Lou et al. (2008) and we determine the Moho depth and mean crustal Vp/Vs ratios below stations from a join analysis of the direct *P* to *S* and corresponding first multiple conversions at the Moho (see below). This approach permits a reliable estimate of the Moho depth however it may result in a slightly offset of shallower and deeper interfaces. We also compared receiver functions migrated cross-sections using two velocity models which conclude to depth variations of the interfaces remain within ±5 km (see Appendix A).

We present the migrated receiver functions along two linear profiles perpendicular to the major geological structures of the area as shown in the Fig. 2.

The constructed section reveals a Moho at ~63 km depth beneath the eastern part of the Tibetan plateau, with a slight thickening towards the Wenchuan fault, whereas it lies at 44 km depth beneath the Sichuan Basin (Fig. 2). This transition occurs over a horizontal distance of less than 30 km, and is located right beneath the Wenchuan strike slip shear zone.

Below the Sichuan Basin a positive interface is observed at ~30 km depth, which represents the top of a high velocity lower crust. Although more complex, a similar lower crustal interface is also visible at 45 km depth west of the surface trace of the Wenchuan fault, above the zone where the Moho is the deepest (Fig. 3). Further west beneath the Tibetan Plateau, no major velocity increase in the middle/lower crust is observed, probably indicating more gradual variations in seismic velocity with depth.

The presence of partial melt within the middle crust of the eastern part of the Tibetan plateau has been advocated based on observations of low mid-crustal seismic velocities and high Poisson ratios (Xu et al., 2007; Wang et al., 2008). The velocity ratio is an important parameter because it provides valuable constraints on crustal composition (Christensen, 1996) and presence of fluids or partial melting inside the crust (Mavko, 1980; Makovsky and Klemperer, 1999). High average crustal Poisson's ration (σ>0.3) is a strong indicator for the existence of partial melting in the crust (Owens and Zandt, 1997). Below each station of our network we compute the average Vp/Vs ratio of the crust from the relative arrival time of the *P*-to-*S* conversion at the Moho and the one from the first multiple reflection PPS (*P* wave reflected first at the free surface at then reflected and converted into *S* wave at the Moho). This can be performed by treating each station individually as proposed by Zhu and Kanamori (2000) or by comparing the migrated sections computed from the PS and the PPS phase as proposed by Kind et al. (2002). We use the approach assuming a constant 1D velocity model with an initial Moho at 70 km depth and we pick the depth of the interface associated with the Moho on both migrated sections (Fig. 4a–b). We then used the depth differences to recover the proper crustal thickness and the average Vp/Vs ratio (Fig. 4c) along the profile assuming a constant crustal Vp of 6.5 km/s. We found an average crustal velocity ratio of about 1.69 (σ=0.23) beneath the Songpan–Garze area which is lower than the mean value for continental areas (Zandt and Ammon, 1995). This observation, along with available estimates of the Poisson ratio further west in the same geological unit (Vergne et al., 2002), does not suggest the existence of a thick and extensive zone of partial melt within the crust beneath the Songpan–Garze Terrane. Moreover, no major velocity increase/decrease associated with the top/bottom of a low velocity zone inside the crust is observed on the migrated images. At the western end of our seismological profile, the high velocity ratio may be interpreted as a consequence of the occurrence of the Xianshuihe fault that separates two different blocks. This high ratio is in agreement with the results of Xu et al. (2007). Underneath the Sichuan basin a mean crustal velocity ratio of about 1.79 (σ=0.27) has been obtained and is interpreted as a result of a high Vp/Vs ratio in

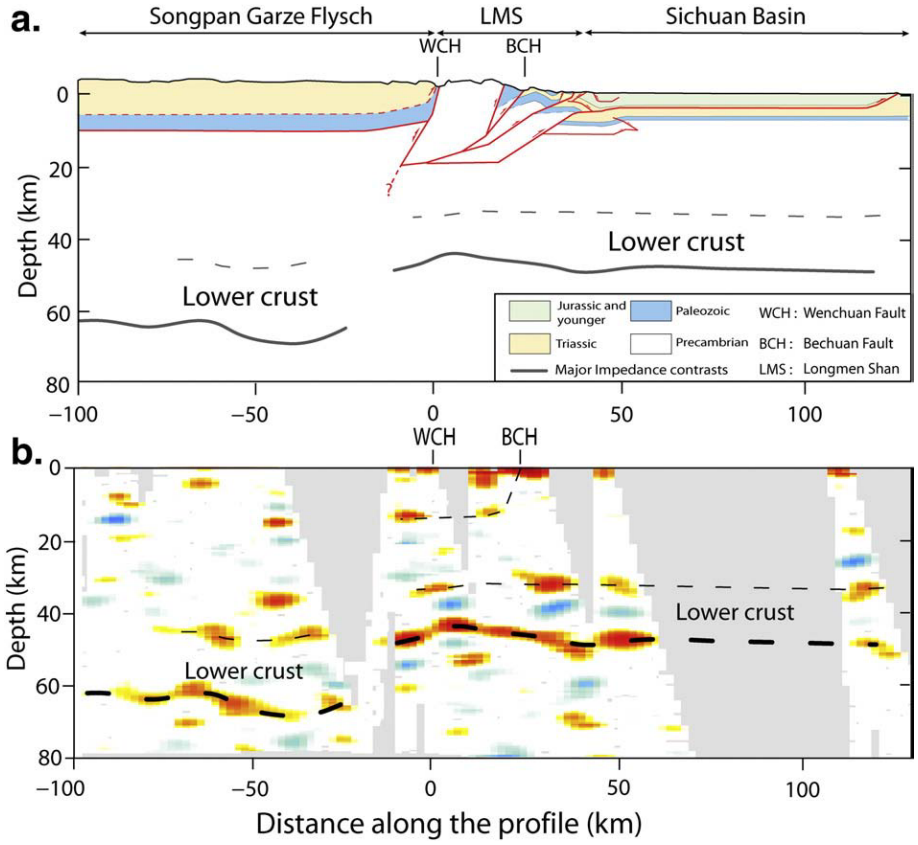

Fig. 3. Combination of geological and geophysical results projected along a single transect following approximately the seismological experiment. (a) Modified geological cross section from Hubbard and Shaw (2009), Burchfiel et al. (2008) and our field observations, (b) Migration of the receiver functions along the geological cross-section. Gray dashed lines indicates major positive impedance contrasts (interfaces) and have been reported on the crustal scale geological cross-section.

Please cite this article as: Robert, A., et al., Crustal structures in the area of the 2008 Sichuan earthquake from seismologic and gravimetric data, Tectonophysics (2009), doi:10.1016/j.tecto.2009.11.010

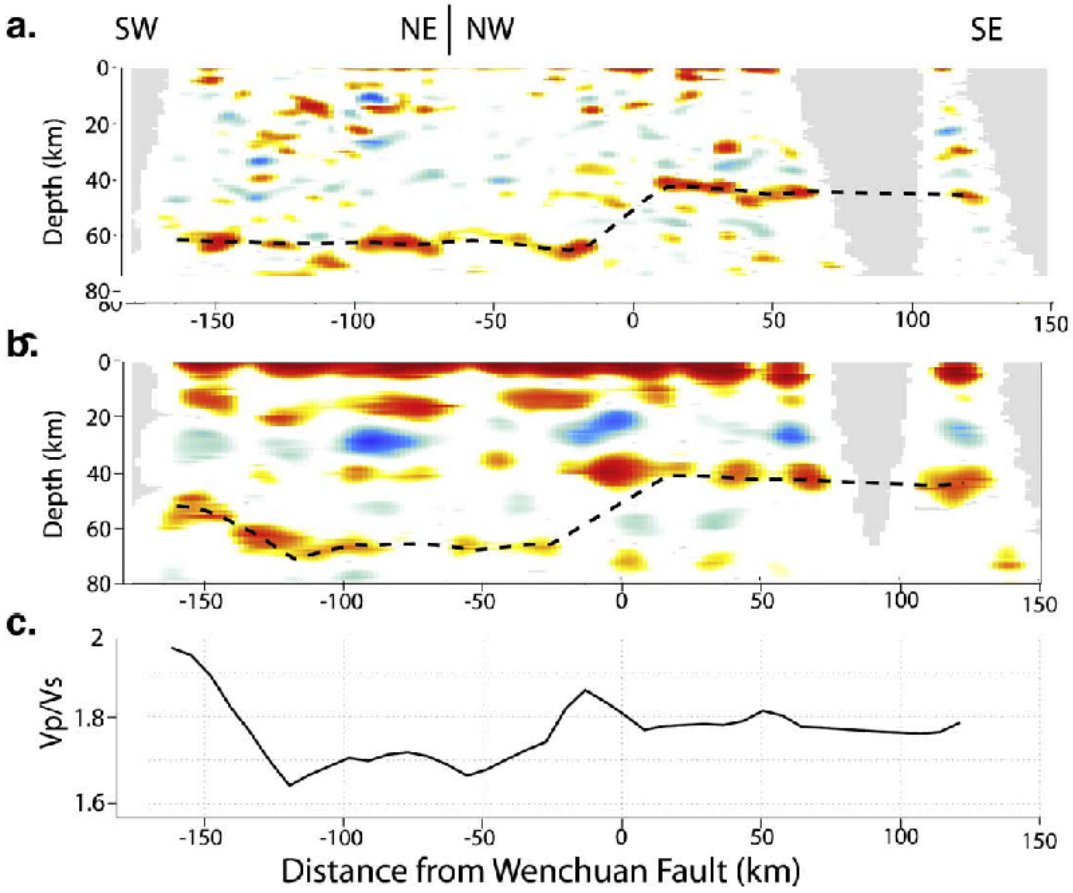

Fig. 4. (a) Receiver functions migration of the PS phases along two profiles sub perpendicular to the Longmen Shan front and to the Xianshuihe fault, with orientations N45 and N135, respectively. Dashed line represents the depth of the Moho picked on PS phases. (b) Receiver functions migration of the first multiple PpPS phase (P wave first reflected at the free surface and then reflected and converted into S wave at depth). Following the approach of Kind et al. (2002). (c) Estimation of the mean crustal Vp/Vs ratio required to explain the picked depths of the Moho on both the PS and PpPS migrations (see Kind et al., 2002, for further details).

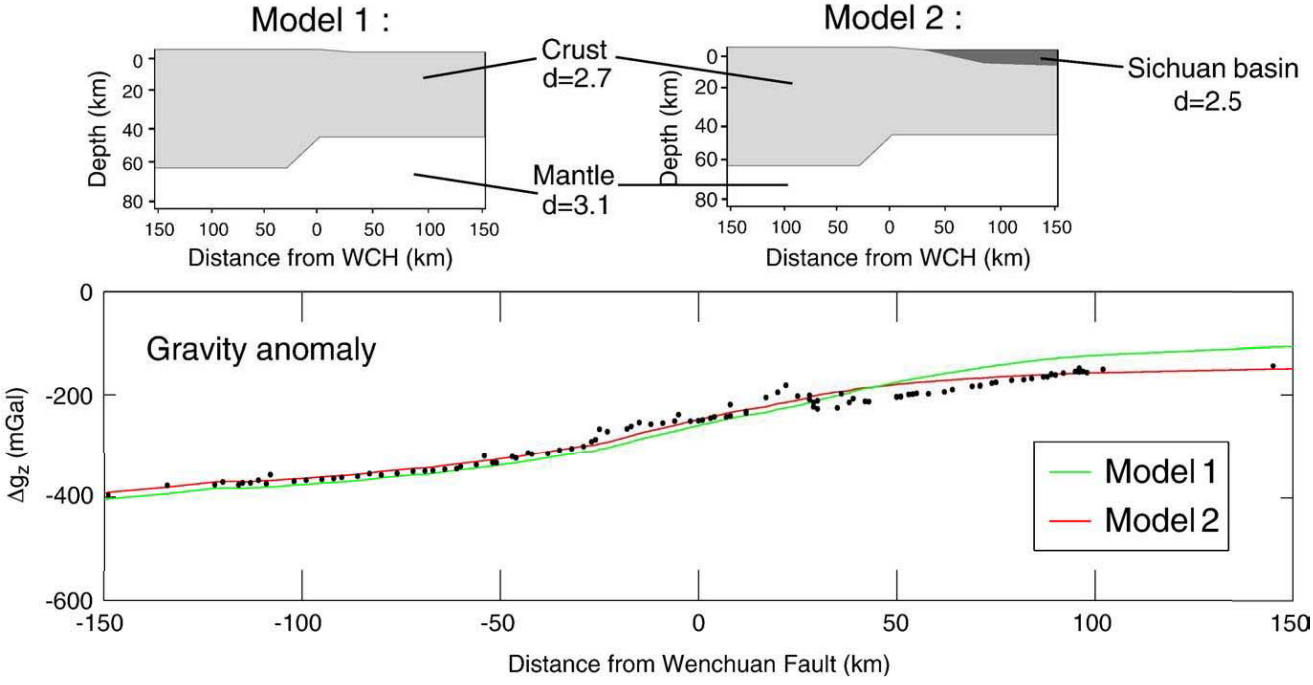

Fig. 5. Gravity data modelling. (a) Density models used to model the gravity anomaly. (b) Black circles indicate gravity anomaly measurements from a dense survey acquired along the transect and completed with regional data (Xu et al., 2007). Green line shows calculated gravity anomaly using a very simple crust/mantle density model in agreement with the geometry inferred from the seismological study. Red line shows the calculated gravity anomaly using common density contrasts and simplified geometries for the Moho and the base of the Sichuan basin.

Please cite this article as: Robert, A., et al., Crustal structures in the area of the 2008 Sichuan earthquake from seismologic and gravimetric data, Tectonophysics (2009), doi: 10.1016/j.tecto.2009.11.010

the Sichuan basin sediments. These results are in agreement with the estimates from receiver function technique of Lou et al. (2008) who obtained a mean crustal velocity ratios of 1.73 ($\sigma = 0.25$) for the Songpan–Garze unit and 1.83 ($\sigma = 0.29$) for the Sichuan Basin.

Within the upper crust, we observe a series of positive converters that form, when connected, a westward dipping interface starting close to surface at the Longmen Shan front and flattening at ~15 km depth beneath the eastern Songpan–Garze Terrane (Fig. 2). The projection of the hypocenter of the 12 May 2008 earthquake, is located very close to this interface (Fig. 2). We propose that the high impedance contrast observed is associated with a decollement shear zone which could correspond to the western continuation of Guanxian–Beichuan–Wenchuan faults system at depth (Fig. 3).

3. Gravity data modelling

We model both the regional gravity field (Jiang and Jin, 2005) and micro-gravity measurements acquired along the seismological profile using geometrical constraints inferred from seismological data and geological data for the upper part of the crust (Burchfiel et al., 2008; Hubbard and Shaw, 2009) (Fig. 5). Geometry of the Moho deduced from seismological study was tested for the gravity anomaly modelling. We use a typical density contrast of 400 kg m^{-3} for the mantle–crust boundary (Holt et al., 1987; Gimenez et al., 2009). The density model 1 shows the signature of the Moho alone and demonstrates that the wavelength of the gravity anomaly is in agreement with a sharp Moho offset. However this simple model underestimates the gravity anomaly east of the Longmen Shan range. This is probably because it does not take into account the low density sediments of the foreland basin that was mainly developed during Trias to Cretaceous. We assume a 200 kg m^{-3} density contrast between the crust and the Sichuan basin inferred from the density log of Sichuan Basin sediments presented in Jiang and Jin (2005). Trying to reduce differences between modelled and observed gravity anomaly, the lower density of sediments associated with the Sichuan basin has been considered in the density model 2. Despite local discrepancies between observed and calculated Bouguer anomalies, this simple density model indicates that the gravity observations are consistent with the 20 km Moho offset observed on the seismological data.

Based only on gravity anomaly (Jiang and Jin, 2005; Burchfiel et al., 2008) have modelled a smooth westward Moho deepening that is not consistent with the Moho geometry deduced from our seismological imaging and is a consequence of the non-uniqueness of the gravity anomaly modelling.

4. Discussion and conclusion

The combined seismological and gravity data suggest that the Guanxian-Beichuan-Wenchuan fault system marks a zone of strain localization at a lithospheric scale. A horizontal distance of ~250 km is commonly reported for the ~25 km Moho deepening across the Himalaya and southeast Tibet, which is explained by the flexure of the Indian crust (Hetenyi et al., 2006). Here, the sharp Moho offset across the eastern margin of the Tibetan plateau cannot be explained with flexural support and rather requires a subvertical discontinuity between the Tibetan lithosphere and the Yangtze craton. Furthermore the deepening of the Moho is not directly located beneath the Beichuan fault where the surface elevation increases abruptly from 1.5 to 3 km, but rather ~30 km westward. The lack of a direct connection between the surface trace of the Guanxian–Beichuan–Wenchuan fault system and the Moho offset can be related to the receiver function technique itself, which cannot show an image of subvertical discontinuity. However based on our results as well as the location of the 12 May 2008 event, we rather interpret this lack of connection in terms of geometry of the Beichuan fault, which may extend subhorizontally at a depth of ~15 km to root along a crustal decollement beneath the Tibetan plateau. The offset between the position of the Guanxian–Beichuan–Wenchuan fault system and the deepening of the Moho is probably the result of the relative strength of the two blocks. We propose that the convergence is accommodated by ductile deformations within the Tibetan lithosphere, the Yangtze craton is acting as a rigid block. Hence, the earthquake of May 12 reflects the brittle deformation of the upper crust.

Acknowledgments

We are grateful to many people who participated in measurements campaign, especially students from the Chengdu University and Southwest Petroleum University. Funding was provided by INSU/CNRS (Relief and Dyeti programs) and ANR grants. Thoughtful reviews from anonymous reviewers significantly improved the manuscript.

Appendix A. Supplementary data

Supplementary data associated with this article can be found, in the online version, at doi:10.1016/j.tecto.2009.11.010.

References

Burchfiel, B.C., Royden, L., van der Hilst, R., Hager, B., Chen, Z., King, R.W., Li, C., Lü, J., Yao, H., Kirby, E., 2008. A geological and geophysical context for the Wenchuan earthquake of 12 May 2008, Sichuan, People's Republic of China. GSA Today 18, 4–11. doi:10.1130/GSATG18A.1.

Burdick, L.J., Langston, C.A., 1977. Modeling crustal structure through the use of converted phases in teleseismic body-wave form. Bull. Seismol. Soc. Am. 67, 677–691.

Chen, Z., Burchfiel, B.C., Liu, Y., King, R.W., Royden, L.H., Tang, W., Wang, E., Zhao, J., Zhang, X., 2000. Global positioning System measurements from eastern Tibet and their implications for India/Eurasia intercontinental deformation. J. Geophys. Res. 105 (B7), 215–227.

Christensen, N.I., 1996. Poisson's ration and crustal seismology. J. Geophys. Res. 101 (B2), 3139–3156.

De Michele, M., Raucoules, D., Lasserre, C., Pathier, E., Klinger, Y., Van Der Woerd, J., de Sigoyer, J., Xu, X., in press. The Mw 7.9, 12 May 2008 Sichuan earthquake rupture measured by sub-pixel correlation of ALOS PALSAR amplitude images. Earth Planets Space.

Dueker, K.G., Sheehan, A.F., 1998. Mantle discontinuity structure beneath the Colorado Rocky Mountains and High Plains. J. Geophys. Res. 103 (B4), 7153–7170.

Gan, W., Zhang, P., Shen, Z.-K., Niu, Z., Wang, M., Wan, Y., Zhou, D., Cheng, J., 2007. Present-day crustal motion within the Tibetan Plateau inferred from GPS measurements. J. Geophys. Res. 112, B08416. doi:10.1029/2005JB004120.

Gimenez, M.E., Braitenberg, C., Martinez, M.P., Introcaso, M., 2009. A comparative analysis of seismological and gravimetric crustal thicknesses below the Andean Region with Flat Subduction of the Nazca Plate. Int. J. Geophys.. doi:10.1155/2009/607458 ID 607458.

Hetenyi, G., Cattin, R., Vergne, J., Nabelek, J.L., 2006. The effective elastic thickness of the India Plate from receiver function imaging, gravity anomalies and thermomechanical modelling. Geophys. J. Int. 167, 1106–1118.

Holt, W.E., Chase, C.G., Wallace, T.C., 1987. Crustal structure from three-dimensional gravity modelling of a metamorphic core complex: a model for uplift, Santa Catalina-Rincon mountains, Arizona. Geology 15, 979–980. doi:10.1130/0091-7613.

Hubbard, J., Shaw, J.H., 2009. Uplift of the Longmen Shan and Tibetan plateau, and the 2008 Wenchuan (M = 7.9) earthquake. Nature 458, 194–197. doi:10.1038/nature07837.

Jiang, X., Jin, Y., 2005. Mapping the deep lithospheric structure beneath the eastern margin of the Tibetan Plateau from gravity anomalies. J. Geophys. Res. 110, B07407. doi:10.1029/2004JB003394.

Kind, R., Yuan, X., Saul, J., Nelson, D., Sobolev, S.V., Mechie, J., Zhao, W., Kosarev, G., Ni, J., Achauer, U., Jiang, M., 2002. Seismic images of crust and upper mantle beneath Tibet: evidence for Eurasian plate subduction. Science 298, 1219–1221.

Ligorria, J.P., Ammon, C.J., 1999. Iterative deconvolution and receiver-function estimation. Bull. Seismol. Soc. Am. 89 (5), 1395–1400.

Lou, H., Wang, C.Y., Lu, Z.Y., Yao, Z.X., Dai, S.G., You, H.C., 2008. Deep tectonic setting of the 2008 Wenchuan Mw8.0 earthquake in southwestern China. Sci. China Ser D-Earth Sci. 52 (2), 166–179.

Makovsky, Y., Klemperer, S.L., 1999. Measuring the seismic properties of Tibetan bright spots: evidence for free aqueous fluids in the Tibetan middle crust. J. Geophys. Res. 104 (B5), 10795–10825.

Mavko, G., 1980. Velocity attenuation in partially molten rocks. J. Geophys. Res. 85, 5173–5189.

Owens, T.J., Zandt, G., 1997. Implications of crustal property variations for models of Tibetan plateau evolution. Nature 387, 37–43.

Richardson, N.J., Densmore, A.L., Seward, D., Fowler, A., Wipf, M., Ellis, M.A., Yong, L., Zhang, Y., 2008. Extraordinary denudation in the Sichuan Basin: insights from low-temperature thermochronology adjacent to the eastern margin of the Tibetan Plateau. J. Geophys. Res. 113, B04409. doi:10.1029/2006JB004739.

Royden, L.H., Burchfiel, B.C., Wing, R.W., Wang, E., Chen, Z., Shen, F., Liu, Y., 1997. Surface deformation and lower crustal flow in eastern Tibet. Science 276, 788–790. doi:10.1126/science.276.5313.788.

Shen, Z.K., Sun, J., Zhang, Y., Wang, M., Bürgmann, R., Zeng, Y., Gan, W., Liao, H., Wang, Q., 2009. Slip maxima at fault junctions and rupturing of barriers during the 2008 Wenchuan earthquake. Nature Geosci. 2. doi:10.1038/NGEO636.

Stone, R., 2008. An unpredictably violent fault. Science 320, 1578.

Tapponnier, P., Zhiqin, X., Roger, F., Meyer, B., Arnaud, N., Wittlinger, G., Jingsui, Y., 2001. Oblique stepwise rise and growth of the Tibet Plateau. Science 294, 1671–1677. doi:10.1126/science.105978.

Vergne, J., Wittlinger, G., Hui, Q., Tapponnier, P., Poupinet, G., Mei, J., Herquel, G., Paul, A., 2002. Seismic evidence for stepwise thickening of the crust across the NE Tibetan plateau. Earth Planet. Sci. Lett. 203, 25–33.

Wang, C., Lou, H., Lü, Z., Wu, J., Chang, L., Dai, S., You, H., Tang, F., Zhu, L., Silver, P., 2008. S-wave crustal and upper mantle's velocity structure in the eastern Tibetan Plateau — deep environment of lower crustal flow. Sci. China Ser. D 51, 263–274.

Xu, L., Rondenay, S., van der Hilst, R.D., 2007. Structure of the crust beneath the southeastern Tibetan Plateau from teleseismic receiver functions. Phys. Earth Planet. In. 165, 176–193.

Xu, X., Wen, X., Yu, G., Chen, G., Klinger, Y., Hubbard, J., Shaw, J., 2009. Coseismic reverse- and oblique-slip surface faulting generated by the 2008 Mw 7.9. Geology 37, 515–518. doi:10.1130/G25462A.1.

Zandt, G., Ammon, C.J., 1995. Continental crust composition constrained by measurements of crustal Poisson's ratio. Nature 374 (6518), 152–154.

Zhu, L., Kanamori, H., 2000. Moho depth variation in southern California from teleseismic receiver functions. J. Geophys. Res. 105 (B2), 2969–2980.

Please cite this article as: Robert, A., et al., Crustal structures in the area of the 2008 Sichuan earthquake from seismologic and gravimetric data, Tectonophysics (2009), doi:10.1016/j.tecto.2009.11.010